

Mechanochemical *versus* sol–gel silica loading of phenolate- and acetate-bridged dizinc complexes: toward instant and inexpensive hybrids for controlled binding and release of Zn^{2+} in pure water†

Taehong Jun, Yonghwang Ha, Jina Kang, Snehadrinarayan Khatua‡ and David G. Churchill*

Received (in Victoria, Australia) 19th May 2010, Accepted 23rd June 2010

DOI: 10.1039/c0nj00381f

Herein, we have explored expeditious and lowered expense SiO_2 -loading in the context of fluorescent “off-on” and “on-off” Zn^{2+} ion detection/controlled release. A simple racemic ligand (H_2rlys) (**1**) prepared *in situ* can be mechanically SiO_2 -loaded so as to induce surface sites that allow for “off-on” aqueous fluorescence ($\lambda_{\text{em,max}} = \sim 450 \text{ nm}$) detection of Zn^{2+} ; with Cu^{2+} as a competing input, “inhibit” logic gate behaviour is present. Oppositely, dimeric, chiral fluorescent zinc complexes ($\Phi_{\text{F}} = \sim 0.20$) prepared in a “one pot” method, and bearing different $\text{Zn} \cdots \text{Zn}$ internuclear spacings, can be incorporated into silica by two methods. Specifically, the chiral $\text{Zn}_2(\text{slysH})_2\text{Cl}_2$ (**2**) and racemic $\text{Zn}_2(\text{rslysH})_2(\mu\text{-OAc})_2$ species (**3**) [*slys* or *rslys* = 6-amino-2-((2-hydroxybenzylidene)amino)hexanoate] were mechanochemically loaded. An adsorption constant was 1.99×10^{-4} (molecules of **2**/units $\text{SiO}_2(\text{min})^{-1}$ for times of 5–20 min, as determined by extensive SEM-EDS data. These confirmed the highly selective “on-off” rapid aqueous fluorescent Cu^{2+} detection (*versus*, Li^+ , Na^+ , Cs^+ , Mg^{2+} , Ca^{2+} , Mn^{2+} , Fe^{2+} , Co^{2+} , Ni^{2+} , Ag^+ , Cd^{2+} , Hg^{2+} , Pb^{2+}) through direct Zn^{2+} displacement under bulk neat water flow ($\text{pH} = 7.4$) as verified by an authentic sample of $[\text{Cu}_2(\text{slysH})_2(\text{NO}_3)_2]\text{-silica}$ (**4-silica**). With the use of **2**· SiO_2 , Na_4EDTA and Cu^{2+} “inhibit” logic gate behaviour was also found. Sol–gel techniques allowed for loadings of **2** (20–890 mg) up to 1 : 1 (by wt). The preparation of these inorganic hybrids are extremely inexpensive and rapid to prepare from commercial starting materials and can be extended to variegated forms of SiO_2 ; alumina gel was also functionalized with **2**. Cu^{2+} and Zn^{2+} are metals pertinent to human neurological health promotion and in neurodegenerative diseases.

Introduction

Silica is a tremendously ubiquitous and versatile material with greatly expanding utility and potential use upon every passing research year. Its hybrid forms and current and emergent applications continue, and are anticipated, to be extensively explored.^{1–5} Silica, in all its multifarious forms and sizes, is generally inexpensive (gel $\geq \sim \$5 \text{ USD kg}^{-1}$) and is important because of its piezoelectric sensing capabilities and inherent chirality (quartz crystals).⁵ Particles of silica can be interfaced with organic- and metal-containing species in a variety of ways to create useful hybrid species. Silica has vastly outdone itself in the sensing realm with the advent of Xerogels that demonstrate versatility in bio- and chemo-recognition as underscored by accomplishments from the laboratory of

F. V. Bright and co-workers,⁶ among others. There is interest in how silica can coincide with molecular sensing efforts toward real medical or environmental applications, through fluorophore incorporation.⁷ While there are a great many medical initiatives reported^{8–10} there is still a paucity of attempts connecting silica capabilities with the growing frontier of neurodegenerative research.^{11–20}

The metal ions Zn^{2+} and Cu^{2+} have been explored herein in the context of SiO_2 functionalization. These ions are commonly of interest in better understanding mechanisms of neurodegeneration; also, there are considerations of environmental remediation (with, *e.g.*, Cu^{2+}). Environmentally safe levels of copper(II) are held at the ppb level ($\sim 1 \times 10^{-9}$). Considering these metals in human neuronal health, zinc(II) is a ubiquitous and vital species, part of the intricate workings of chemical (*vis-à-vis*, electronic) neurotransmission. It can be found, for instance, to strongly bind to protein histidines.²¹ The importance of the soluble free (*versus* complexed) cupric ion has enormous natural consequences that cannot be understated in, *e.g.*, neurodegeneration through its binding as well as its redox nature. The homeostasis of biological copper species involves a delicate balance of a variety of natural transporters and biological processes. When there is disruption to human metal ion homeostasis, pathology may

Molecular Logic Gate Laboratory, Department of Chemistry, Korea Advanced Institute of Science and Technology (KAIST), 373-1 Guseong-dong, Yuseong-gu, Daejeon, 305-701, Republic of Korea. E-mail: dchurchill@kaist.ac.kr; Fax: +82 42-350-2810; Tel: +82 42-350-2845

† Electronic supplementary information (ESI) available: Reproductions of SEM-EDS data reports, plots and related data. See DOI: 10.1039/c0nj00381f

‡ Current address: Universität Siegen, OCI Siegen, NRW, 57076, Germany.

present in forms that include serious neurodegenerative diseases such as Wilson's disease, Alzheimer's disease and prion-induced diseases.^{22–25} Environmentally, free Cu^{2+} is considered an environmental pollutant, in, *e.g.*, drinking²⁶ and river water.²⁷ Thus, the development of Cu^{2+} -oriented silica-based molecular probes²⁸ and those for other “heavy” metals that interface with aqueous solutions continues unabated as a research topic of considerable interest in analytical and biological chemistry.

Metal complexation of zinc and copper ions with given artificial ligands (receptors) and a consideration of their varying binding abilities have involved intense research. Simply, the Irving Williams series and the notion that Cu^{2+} is a “universal quencher” are basic tenets in receptor design. Ligands that are developed for solutions and which are

employed in hybridized materials often retain these same properties in molecular recognition systems. There are various reports involving fluorescent metal ion recognition with silica; importantly, aqueous environment Cu^{2+} has been addressed before with respect to silica-based sensing platforms.^{26,29} More specifically, there are Schiff base complexes of Zn^{2+} already reported for SiO_2 -based or SiO_2 -related systems.^{30–33}

This research group has previously pursued novel means of sensing and host–guest recognition,^{34–37} and chirality of small molecules that might be used practically as receptors in the realm of diagnostics or therapy in neurodegenerative research.³⁸ In recent times, this laboratory has reported interesting chiral dizinc and dicopper Schiff base complexes (Fig. 1) for investigations into efficient means of chemical and/or ion recognition.^{39–41} As detailed atomic level characterization and analyte binding studies are already reported for compounds **2–4**, we now explore the behavior of these species on solid supports. These systems have not yet been considered in terms of molecular logic gating function in which chemical species (*e.g.*, metal cations, bio(in)organic ions) serve as external stimuli (IA, IB) and an optical signal (UV-vis absorption and or fluorescence emission) is the reporting output (Q).^{39–41} Some recent papers pertaining to silica (particles) have featured systems that can exhibit optical behavior that can be interpreted in terms of logic gating.^{42–46}

This brings us to the means of forming silica hybrids. Specifically, mechanochemical loading is rapid and can easily be quantified, as explored herein, and allows us to approach some concepts of SiO_2 -hybridization for compounds **1–4** in terms of (i) a comparison of different grinding conditions, (ii) a comparison between mechanical loading and sol–gel techniques (Scheme 1), (iii) a comparison between recognition with addition of Zn^{2+} , (iv) the involvement of two Zn^{2+} dimers bearing different intermolecular $[\text{Zn} \cdots \text{Zn}]$ distances, and (v) the future possibility of controlled artificial zinc uptake and release (artificial zinc transport).^{47,48}

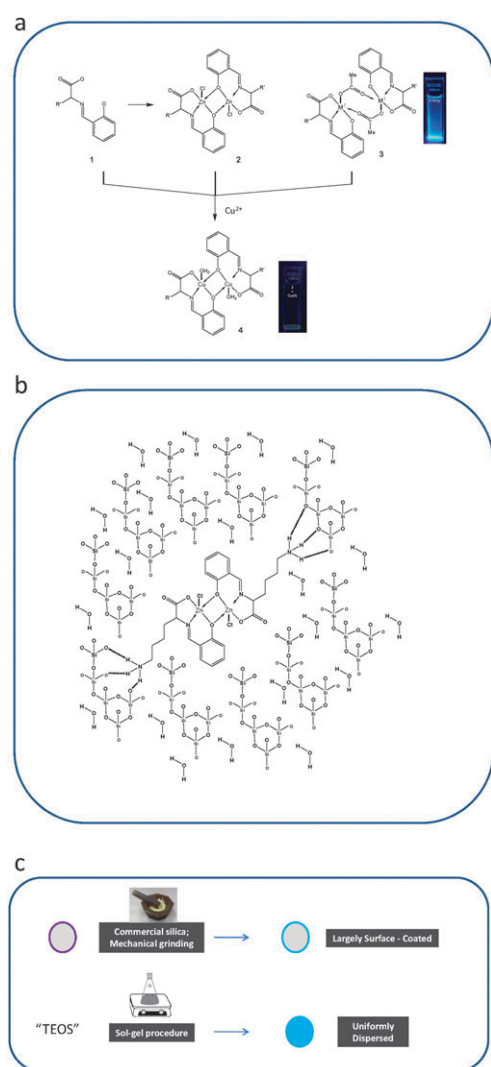
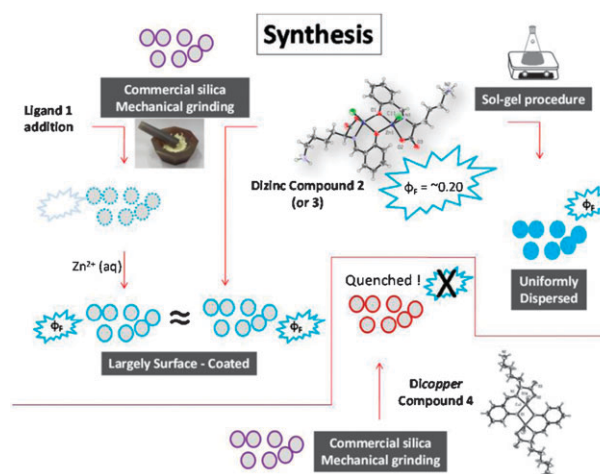


Fig. 1 (a) Structures of ligand **1** and dizinc compounds **2** and **3** tested herein arranged in an ideal scheme whereby the copper dimer species **4** is produced, $\text{R}' = (-\text{CH}_2\text{CH}_2\text{CH}_2\text{CH}_2\text{NH}_3\text{Cl})$. (b) Cartoon of possible complex silica interactions at the available layer after surface loading or sol–gel combination. (c) Cartoon of two types of processing showing favor for surface loading from mechanical grinding or from the sol–gel allowing for a more uniform coating.



Scheme 1 Cartoon of the various types of silica loading pursued herein using compound **1**, the two types of dizinc species (compounds **2** and **3**) and the authentic quenching dicopper species (compound **4**).

Results and discussion

Mechanochemical formation of 1-silica, 2-silica, 3-silica, and 4-silica

First, mechanochemical synthetic additions of compounds **1–4** to commercial silica gel will be discussed. We have prepared a hybrid-type material through the use of commercially available silica gel (*vide supra*) and through using prepared silica gel and a Schiff base ligand (compound **1**), fluorescent dizinc species (compounds **2** and **3**), or a dicopper complex (compound **4**) that has been previously obtained (Scheme 1). First, the crude ligand (**1**) was prepared and isolated; it was combined with silica to give a hybrid that, upon workup, has the capability of binding metals into the Schiff base sites. This can be determined qualitatively by naked eye sensing for various metals independently in solution (Li^+ , Na^+ , Cs^+ , Mg^{2+} , Ca^{2+} , Mn^{2+} , Fe^{2+} , Co^{2+} , Ag^+ , Ni^{2+} , Cd^{2+} , Hg^{2+} , and Pb^{2+}). The turn-on effect is clear in Fig. 4. Compound **4** [$\text{Cu}_2(\text{slys})_2(\text{OH})_2$] can be mechanically loaded as well, to achieve an authentic sample that gives no fluorescence.

Obtaining the adsorption constant

Longer grinding times should effect greater surface loading. This was explored with compound **2**. With respect to **2**-silica, the most important point is that more of compound **2** can be mechanochemically loaded given more grinding. For **2**, the “grinding constant” was determined to be 1.99×10^{-4} (molecules of **2**/units $\text{SiO}_2(\text{min})^{-1}$, for the time range 5–20 min explored herein, from the slope of a straight line fit through the data points in a graph of the ratio of Si-to-Zn as a function of the mechanical grinding time (*t*) (Fig. 2). This plot involves standard deviation hash marks; for the four data points, each value was repeated 2–3 times and is an average of 6–9 SEM-EDS point trials. For a graph that bears error bars signifying experimental error, see the ESI.† Some saturation appears to be present for the Si-to-Zn value at $t = 20$ min. This constant is thought to reveal partly the type of compound

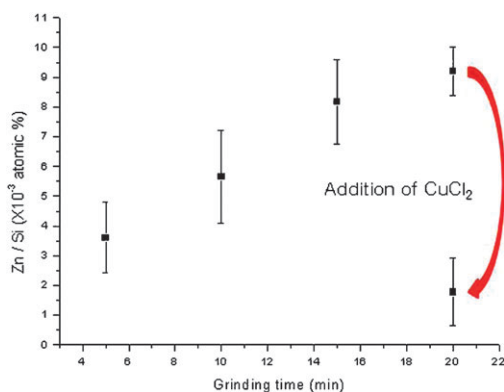


Fig. 2 Graph of Si-to-Zn atomic content ratios (SEM-EDS) as a function of mechanical grinding time (mortar and pestle) in minutes with prepared polydispersed silica nanoparticles. Standard deviation bars for each data point are derived from 6–9 EDS values from sampling of the same sample. A straight line fit gives a “grinding constant”: 1.99×10^{-4} (molecules of **2**/units $\text{SiO}_2(\text{min})^{-1}$. A sudden drop in the Zn/Si ratio occurs upon addition of Cu^{2+} (10 mL, 10^{-2} M CuCl_2 solution).

being adsorbed and the molecular forces that exist between **2** and silica. However, this value may also be jointly involved with the production of a larger amount of surface area *via* any pulverization of silica that ensued, since further particle division would likely scale with longer grinding times. Such possible inadvertent effects were not further considered herein. Further, mechanical loading constants such as the one obtained above may vary under other conditions that relate to the type of dye molecule, the size and type of silica, the level of mechanical pressure, *etc.* Such parameters and aspects will be interesting to study in the future.

Characterization and properties of mechanically mixed hybrid material **2**-silica

The purpose of mechanochemical combinations is to explore the utility of this avenue which can be considered part of green chemistry, and in investigations of potential artificial Zn^{2+} transporting systems. The composite [$\text{Zn}_2(\text{slysH})_2\text{Cl}_2$]-silica (**2**-silica) can thus be tested for its resilience and robustness. First, we wanted to determine whether compound **2** or **3** is retained on *thoroughly* washed material; visually, the fluorescence of the silica appears the same as that for the solution of compound **2** or **3**. There is also a distinct signal imparted by Zn^{2+} in all silica-hybrid samples. These hybrid materials can be heated as dry solids at 80°C for 1.0 week, after which time they maintain the same level of fluorescence. Further, samples of this functionalized silica can be boiled in neat distilled water for 1.0 day, again with excellent retention of blue fluorescence; importantly, the water phase did not attain any degree of blue fluorescence. Furthermore, the **2**-silica materials can be washed liberally with neat methanol or ethanol, also, without apparent disruption of the **2**-silica material. **2**-silica does, however, degrade in the presence of strong Brønsted acids such as concentrated HCl solution (~ 10 M). While commercial silica gel 60 (0.040–0.063 mm) was used herein, the type, size, or form of silica may impart different effects or surface coverage. Additionally, loading **2** onto alumina particles (0.063–0.200 mm Merck), as well, shows retention of fluorescence derived from the molecular properties of **2**, suggesting that the adsorption environment does not change significantly.

In terms of a molecular view of the interactions between, *e.g.*, compound **2** and the silica surface, the depiction in Fig. 1 (a working model) reveals a presumably great degree of hydrogen bonding between the derivatized lysine side-chain termini and silica oxygen atoms (Fig. 1b). The characterization of the coordination sphere (number and type of donor atoms) of Zn^{2+} through XAFS will be an important part of our future work, but it has its limitations in that it might not discern the difference between a Si–O or H_2O axial oxygen donor atom bound to Zn^{2+} . Separately, while the anion on **2** can vary, perchlorates in particular must not be used because of the need to grind the material.⁵¹ [The presence of a (i) ligand that involves a nitrogenous base(s) (reductant), (ii) perchlorate (oxidant) and (iii) mechanical grinding (initiator) might be enough to cause an unexpected detonation (*i.e.*, the fire triangle) under some conditions.] These hybridization studies can be extended to other solvents or solvent mixtures, but

importantly are studied in aqueous media for consideration in real-case waste streams.

Solution sol–gel method with $\text{Zn}_2(\text{slysH})_2\text{Cl}_2$

For comparison of different modes of mixing, a separate $\text{Zn}_2(\text{slysH})_2\text{Cl}_2$ hybrid using conventional sol–gel techniques was performed (Scheme 1). This process is an adaptation from a well known literature procedure,⁵⁰ but has never been performed with **2**, **3** or like molecules. Silica nanoparticles were generated by the sol–gel process in which a portion of TEOS was dissolved in an ethanol–water mixture over a range of solid weight ratios of **2** (Fig. 3). Specifically, an ammonia solution was added to the stirring reaction mixture of TEOS and compound **2** solution which was later allowed to stand at room temperature for 1.0 days. A white precipitate formed that was able to be conveniently isolated by centrifugation (6000 rpm \times 30 min \times 3–4 repetitions) and determined to be silica nanoparticles *via* characterization using SEM-EDS. The nature of the material was elucidated by inspection of SEM images revealing highly clustered particles of size \sim 100–250 nm. This material allows for comparative results with the mechanically ground samples from commercial silica. Importantly, both samples are prominently blue-fluorescent and respond significantly to Cu^{2+} addition in a fluorescent on–off fashion.

Testing 1–silica with addition of Zn^{2+} (aq)

The inherent fluorescence of the zinc species (**2** and **3**) allowed us to form zinc monomers or dimers as we add zinc(II) ions to an aqueous suspension of the ligand-functionalized silica (**1**–silica). “Before and after” photographs of this are shown in Fig. 4, in which the ligand itself (Fig. 4, left side), which is mildly fluorescent, undergoes a multi-fold increase upon Zn^{2+} binding (excess Zn^{2+} addition).

In terms of potential logic gating interpretations of the changes in optical signals with respect to chemical inputs, an interpretation is shown in Table 1. The substrate is the **1**–silica hybrid, with Zn^{2+} and Cu^{2+} designated as inputs *A* and *B*, respectively. The presence of *A* in the absence of *B* is the only case in which there is an output ($\lambda_{\text{ex}} = 365$ nm). While this

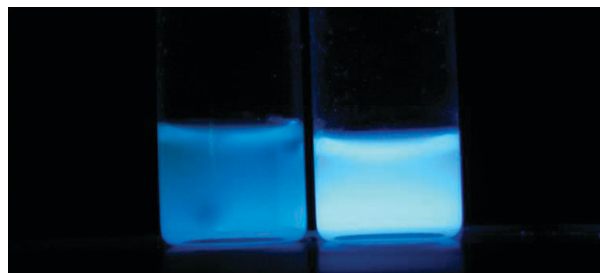
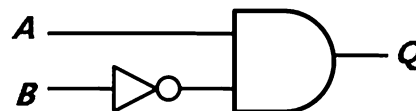


Fig. 4 Digital photo of glass vials containing mechanically ground hybrid H_2slys –silica (**1**–silica) suspended in water under UV irradiation (lamp $\lambda_{\text{ex}} = 365$ nm). (left) Absence of Zn^{2+} ; (right) presence of Zn^{2+} , $[\text{Zn}^{2+}] = \sim 1 \times 10^{-3}$ M.

Table 1 *Inhibit* logic gating (shown symbolically) and a truth table for substrate **1**–silica, with Zn^{2+} and Cu^{2+} as inputs *A* and *B*, respectively (at 1×10^{-3} M), giving optical output *Q*

Input <i>A</i> [Zn^{2+}]	Input <i>B</i> [Cu^{2+}]	Output <i>Q</i> ($\lambda_{\text{em,max}} = \sim 450$ nm)
0	0	0
0	1	0
1	0	1
1	1	0

analysis is quite straight forward, we hope to study more complex systems later.



Addition of M^{2+} and quenching with Cu^{2+}

Next we can consider the effect that soluble metal ions might have on the fluorescence of **2**–silica species. Various metal ions were separately tested (Li^+ , Na^+ , Cs^+ , Mg^{2+} , Ca^{2+} , Mn^{2+} , Fe^{2+} , Co^{2+} , Ag^+ , Ni^{2+} , Cd^{2+} , Hg^{2+} , and Pb^{2+}). However, as was reported for **2** in solution,³⁹ herein on silica there was a great fluorescence decrease exclusively for $[\text{Cu}^{2+}]$. Thus, **2**–silica succumbs to quenching on silica as it does in solution suggesting that it exists adsorbed in a way that allows for facile displacement of Zn^{2+} ions from the Schiff base ligand environment. Fe^{2+} and Co^{2+} do also exhibit fluorescence quenching, but are limited when compared with the effect that Cu^{2+} has.³⁹ A real situation is emulated with a single bulk H_2O flow over silica on a filter paper as emulated by a significant amount of water-containing copper(II) introduced *via* a large funnel suctioned by vacuum filtration. This was operated normally allowing for rapid flow-through (rate ≈ 1.0 L min^{-1}). More accurate assays could be made when studying the optical changes in 10 mL vials: additions of a range of M^{n+} species reveal that Cu^{2+} exhibits immediate quenching with, *e.g.*, a 20 mg sample of **2**–silica prepared from a 1 : 1, silica : **2** ratio (by wt) with 20 min grinding. Thus, Zn^{2+} was cleanly displaced from its ligated place in the $\text{Zn}_2(\text{slysH})_2\text{Cl}_2$ –silica hybrid (**2**–silica) upon the presence of Cu^{2+} as shown in Scheme 2. This process is portrayed dramatically in a movie (see ESI†). This behavior is

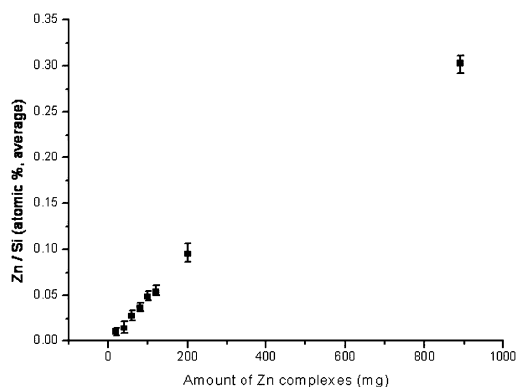
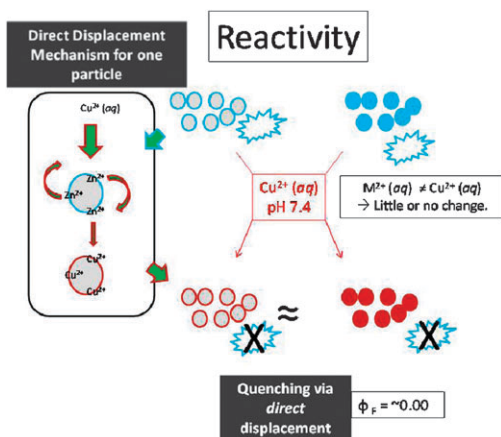


Fig. 3 Graph of the average Zn/Si atomic percentage ratio relating to the difference between the number of $\frac{1}{2}$ compound **2** and SiO_2 units. The graph is a function of the experimental masses for complex **2** upon various loadings (20–890 mg) with consistent use of a 890 mg sample of silica.



Scheme 2 A cartoon of the loss of fluorescence for the two different $\text{Zn}_2(\text{slysH})_2\text{Cl}_2$ -silica hybrids prepared *via* different synthetic procedures (mechanochemical: grey circle with a blue outline; and sol-gel: solid light blue); the same displacement mechanism upon Cu^{2+} addition is invoked under analogous conditions (neat water, RT, pH = 7.4).

additionally conveniently captured *via* before/after photographs, and the contents of the resulting material are quantified by SEM-EDS data (for a sample, see Fig. 5). Specifically, a 2-silica sample derived from 20 minutes of grinding averages a value of ~ 0.009 Zn atom/Si atom ratio,

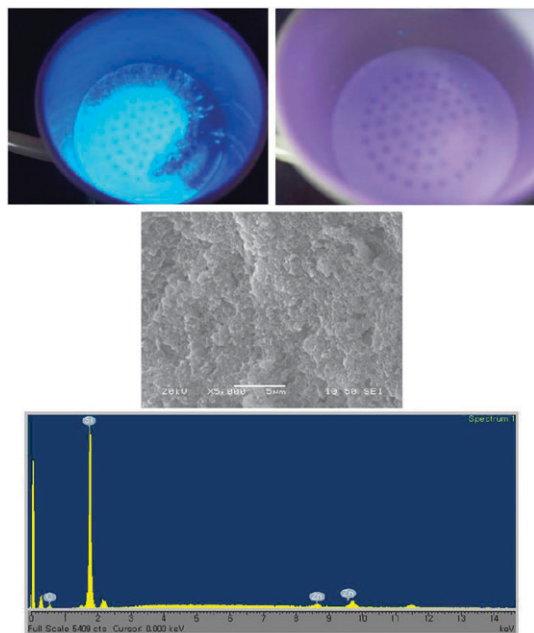


Fig. 5 (top left) Photo of a very recently prepared silica-loaded $\text{Zn}_2(\text{slysH})_2\text{Cl}_2$ (2-silica) exhibiting blue fluorescence ($\lambda_{\text{ex}} = 365$ nm) after thorough H_2O rinsing; (top right) the same sample of silica shortly (<1 min) after macroscale aqueous Cu^{2+} through-flow (1 L; 0.002 M Cu^{2+}) was performed, as detected by optical changes under UV light (also $\lambda_{\text{ex}} = 365$ nm). (middle) Sample SEM image of newly ground 2-silica after a given time; (bottom) EDS spectral measurement assessing the element type (O, Si, Zn) and percent element weight composition in the analyzed material: elemental weight%, atomic%: O (K): 66.85, 78.10; Si (K): 32.71, 21.77; Zn (K): 0.44, 0.13. See ESI† for comprehensive data and numerous diagrams.

Table 2 A diagram of substrate 2-SiO₂ giving input logic gate behavior of “Na₄EDTA inhibits Cu^{2+} ” with an output of $\lambda_{\text{em,max}}$ at ~ 450 nm. Na₄EDTA and Cu^{2+} can be present at various concentrations

Input A [Na ₄ EDTA]	Input B [Cu ²⁺]	Output Q (quenching of $\lambda_{\text{em,max}} = \sim 450$ nm)
0	0	0
0	1	1
1	0	0
1	1	0

but this decreases to a value of 0.001769 upon Cu^{2+} addition. This suggests Zn^{2+} ions are displaced but may be still sequestered elsewhere in the SiO₂ matrix after dislodging; also there may exist a miniscule, but finite value for background Zn^{2+} .

In this case, the optical output is reversed in which there is now quenching at $\lambda_{\text{em}} = \sim 450$ nm in which Cu^{2+} again serves as the inhibitor for the input pair (I_A and I_B). The interpretation of “inhibit” logic gating with Cu^{2+} and Na₄EDTA is shown in Table 2.

The dizinc diacetate compound (3) can also be used in the same context as that found for compound 2 for all of the various aspects explained above. Specifically, compound 3 was hybridized through the use of commercial silica, and also by silica nanoparticles prepared herein. These two different trials gave similar results by inspection of SEM-EDS data (ESI†). Also, similar behaviour in terms of Zn^{2+} displacement with Cu^{2+} was demonstrated. Hybrid versatility can be pursued through further analyte binding studies to clarify whether there are additional, and more subtle fluorescent responses in the context of, *e.g.*, PPI sensing.⁴⁰ A direct hybrid comparison would then bring to the forefront the real utility of the difference of Zn···Zn spacing, as determined by single crystal X-ray diffraction of 3.20 Å for compound 2, *versus* that of 4.02 Å for compound 3. The question of molecular stability between the adsorbed molecules 2 and 3 may also later be brought forward. Also, in subsequent studies, the binding of Zn^{2+} species to alumina was performed (see ESI†). There are no reports of the addition of dizinc phenolate- or acetate-bridging species onto silica yet, to the best of our knowledge. As more versatile behaviour of compounds 1–4 in solution is discovered, this could be examined on silica surfaces as well.

Conclusions

In this contribution we have prepared and investigated novel Schiff base-silica hybrids 1-silica to 4-silica embracing the idea of developing a selective zinc uptake-release system that functions in pure aqueous media under physiological pH. First, we have utilized a ligand (H_2slys) that allows for “off-on” zinc sensing through facile addition of it to silica particle (commercial or sol-gel prepared) surfaces so to give a functionalized surface of silica (1-silica) *via* mechanochemical addition. Further, we added a (chiral) fluorescent dizinc species onto silica (commercial or sol-gel prepared) in order to form a hybrid material ($\text{Zn}_2(\text{slysH})_2\text{Cl}_2$ 2-silica; $\text{Zn}_2(\text{rslysH})_2(\mu\text{-OAc})_2$ 3-silica) for Cu^{2+} sensing in the same “on-off” manner. We have also endeavored to address Cu^{2+} detection herein. Cu^{2+} and Zn^{2+} are metals pertinent to

human neurological health and disease. Taken all together these studies successfully assessed the concept of prospective controlled release of Zn^{2+} , albeit at relatively high Cu^{2+} concentration. Further, **2**-silica also acts as a potential sensing probe for Cu^{2+} ions *via* direct M^{n+} displacement. As in solution, the binding of Cu^{2+} at silica is selective, allowing for analyte detection in the presence of competitive non-transition and transition-metal ions alike. In terms of the silica functionalization procedure, the mechanical loading of complex **2** was effected and can be compared at various times. This *mechanochemical* means allowed for combination with complexes **1–4**; with compound **2**, it can be compared to conventional sol-gel combinations with **2** (in various ratios). Extensive SEM-EDS data were obtained for characterization and, among other things, to quantify a mechanochemical adsorption constant of 1.99×10^{-4} (molecules of **2**/units $\text{SiO}_2(\text{min})^{-1}$ for times of 5–20 min, as determined through SEM-EDS data. These aspects can also be extended to alumina, or possibly to a wider variety of materials that allow for chemisorption or physisorption. When considering the pairs (i) Zn^{2+} and Cu^{2+} or (ii) Na_4EDTA and Cu^{2+} as logic inputs *A* and *B*, “*inhibit*” logic gating is found. In the future, the presence of molecular chirality in these materials is of interest to pursue in targeting the detection of chiral anions and biomolecules. Mechanochemical adsorption is a different dimension to the sol-gel process that involves simple workup conditions.

Experimental

Materials and physical measurements

Materials. All chemicals used herein were used as received from commercial suppliers (Aldrich, Junsei, Merck, and Sigma companies) with no further purification prior to use. Tetraethyl orthosilicate 95% (TEOS) and ammonia solution 28–30% (by mass) were obtained from Junsei chemical. Ethanol 99.9% was purchased from Merck. L-Lysine monohydrochloride 98% was obtained from Sigma. Salicylaldehyde 98% was purchased from Aldrich. Zinc chloride 98% was obtained from Sigma-Aldrich. Silica Gel 60 (0.040–0.063 mm) and Alumina (aluminum oxide, 90 active, neutral) came from Merck.

Instruments/instrumental details. The centrifuge used was a Combi-514R manufactured by Hanil Science Industrial. Centrifugation conditions used were 6000 rpm for 30 min, repeated 2–3 times. SEM-EDS analysis was performed at the *Water Research Laboratory* of Jungwon University (Goesan-gun Chungbuk 367–805, Republic of Korea). Specification of the SEM-EDS (Scanning Electron Microscopy–Energy Dispersive X-ray Spectroscopy) instrumentation is as follows: SEM-Model # JSM6380, JEOL, Japan, year purchased: 2005; EDS: Model # 7582, Oxford instruments England, purchasing year, 2005. The hand-held UV lamp used was a Vilber Lourmat (model # VL-4-LC). Digital photographs of cuvettes, *etc.* for intended naked eye colorimetric/fluorometric detection of Cu^{2+} were taken using a Samsung VLUU NV4 digital camera.

Preparation of the rlysH₂-silica hybrid [1-silica] *via* mechanochemical methods using commercial silica gel

A crude portion of rlysH₂ was synthesized using salicylaldehyde and L-lysine monohydrochloride in methanolic solution.^{39,40} Then, a portion of this prepared ligand mixture (50.0 mg, 0.204 mmol) was combined with a small portion (50.0 mg, 0.832 mmol) of commercial silica (Silica Gel 60, 0.040–0.063 mm, Merck) and rlysH₂ through the use of a medium-sized mortar (inner diameter = 5.1 cm) and matching pestle for 15.0 min. The mortar and pestle were hand-operated under continued, even, pressure for the exact said interval ± 5 s giving a bright homogeneous looking yellow, yet moist, powder after this grinding time. Then, a suction filtration was prepared whereupon the product was washed liberally ($3 \times \sim 300$ mL) with distilled water for removal of any unadsorbed rlysH₂ (compound **1**). While the material is ready for use, sample drying is important for obtaining SEM-EDS analysis. Thus, the material can be vacuum-dried for ~ 10 min, or dried for 1–2 days under ambient conditions. The newly-formed silica material (**1**-silica) retains a *weak* blue fluorescence of the adsorbed ligand. The UV irradiation, through the use of a lamp (photo, Fig. 5), demonstrates “off-on” fluorescence responses with Zn^{2+} as illustrated (photo, Fig. 5, and Movie file, ESI†).

Preparation of Zn₂(slys)₂Cl₂-silica [2-silica] hybrid *via* mechanochemical methods using commercial silica gel

$\text{Zn}_2(\text{slysH})_2\text{Cl}_2$ was synthesized following the reported method using ZnCl_2 , salicylaldehyde and L-lysine monohydrochloride in methanolic solution.^{39,40} Mechanochemical methods using commercial silica gel variable ratios were studied *vide infra*. A small portion (*e.g.*, 50.0 mg, 0.832 mmol) of commercial silica (Silica Gel 60, 0.040–0.063 mm, Merck) and compound **2** [$\text{Zn}_2(\text{slys})_2\text{Cl}_2$] (50 mg, 0.061 mmol) were taken into a medium-sized mortar (inner diameter = 5.1 cm). This solid mixture was ground together mechanically with a matching pestle (dry, room temperature) (Scheme 1) for various timed intervals (5.0, 10.0, 15.0, and 20.0 min). These trials were repeated 2–3 times with 6–9 point sampling from SEM-EDS. The mortar and pestle were hand-operated under continued, even, pressure for the exact said intervals (± 5 s). The effect was the formation of a bright homogeneous looking yellow, yet moist, powder after the requisite grinding. Then, a suction filtration was prepared whereupon the product was washed liberally with distilled water for removal of the portion of $\text{Zn}_2(\text{slysH})_2\text{Cl}_2$ (compound **2**) that did not physisorb to the surface *via* mechanical combination. Traces of bright blue fluorescence observed in the filtrate are lessened to zero with further washing when inspected with a UV lamp ($\lambda_{\text{em}} = 365$ nm). While the material is ready for use in water, sample drying is pursued for obtaining quality SEM-EDS analysis. Thus, the material can be vacuum dried for at least ~ 10 min or dried for 1–2 days in air. The newly formed silica material (**2**-silica) retains bright blue-fluorescence from the adsorbed complexes. Upon UV irradiation (photo, Fig. 5), an “on-off” fluorescence response with Cu^{2+} is exhibited as illustrated (photo, Fig. 5, and Movie file, ESI†).

Preparation of $\text{Zn}_2(\text{rslysH})_2(\mu\text{-OAc})_2$ –silica hybrid [3–silica] *via* mechanochemical methods using commercial silica gel

$\text{Zn}_2(\text{rslysH})_2(\mu\text{-OAc})_2$ was synthesized using $\text{Zn}(\text{OAc})_2$, salicylaldehyde and L-lysine monohydrochloride in a methanolic solution. The detailed preparation of $\text{Zn}_2(\text{rslysH})_2(\mu\text{-OAc})_2$ has been made and has been reported separately.⁴⁹ A small 1 : 1 (by wt) portion (*e.g.*, 50 mg, 0.832 mmol) of commercial silica (Silica Gel 60 (0.040–0.063 mm) Merck) and $\text{Zn}_2(\text{rslysH})_2(\mu\text{-OAc})_2$ (50 mg, 0.067 mmol) were taken into a medium-sized mortar (inner diameter = 5.1 cm) (photo, Fig. 1). This solid mixture was ground together mechanically with an appropriate pestle (dry room temperature) (Scheme 1) for 10 min. These trials were repeated 2–3 times and involved a 6 to 9 point sampling with SEM-EDS. The mortar and pestle were hand-operated under continual, and even, pressure for the exact said time ± 5 s. The effect was the formation of a bright homogeneous-looking yellow powder as described for **2**. Then, a suction filtration apparatus was prepared whereupon the product was washed liberally with distilled water to allow for removal of unadsorbed portions of compound **3**. Traces of fluorescence (bright blue) in the filtrate are lessened to zero by inspection with a UV lamp ($\lambda_{\text{excit}} = 365$ nm). Sample drying and SEM-EDS analysis were carried out in the same way as above. The silica material (**3**–silica) retains a bright blue fluorescence from the adsorbed material when viewed under UV irradiation (photo, Fig. 5), and has an “on–off” fluorescence response when in the presence of Cu^{2+} .

Preparation of unfunctionalized silica nanoparticles

This procedure involved the use of TEOS and was adapted from the Stöber-type literature method.⁵⁰ This material was worked up through the routine use of ultra-centrifugation and isolation to allow for fresh material for combination with metal complexes **2**–**4** described below. SEM-EDS data revealed the formation of individual particles with diameters of 100–250 nm. The presence of some much smaller particles estimated at diameters of ~ 10 nm was observed. All “particles” appeared greatly aggregated.

Preparation of $\text{Zn}_2(\text{slysH})_2\text{Cl}_2$ –silica [2–silica] hybrid *via* mechanochemical methods using synthesized silica nanoparticles

$\text{Zn}_2(\text{slysH})_2\text{Cl}_2$ was synthesized as previously reported *via* a method using ZnCl_2 , salicylaldehyde and L-lysine monohydrochloride in methanolic solution.^{39,40} A small portion of synthesized nanoparticles (see above) (50.0 mg, 0.832 mmol) and $\text{Zn}_2(\text{slysH})_2\text{Cl}_2$ (50 mg, 0.061 mmol) were taken into a small mortar. This solid mixture was then ground together mechanically using a matching pestle (Scheme 1) for various timed intervals (5.0, 10.0, 15.0, and 20.0 min) (humidity $\approx 40\%$, room temperature). These trials were repeated 2–3 times with 6–9 points of sampling *via* SEM-EDS. The mortar and pestle were hand-operated under continued, even, pressure for the said times (± 5 s). The effect was the formation of a bright homogeneous-looking yellow, yet moist, powder after the requisite grinding. Then, a suction filtration was prepared whereupon the product was washed liberally with distilled water to effect removal of unadsorbed $\text{Zn}_2(\text{slysH})_2\text{Cl}_2$

(compound **2**). Traces of bright blue fluorescence in the filtrate are lessened to zero by inspection with a UV lamp ($\lambda_{\text{em}} = 365$ nm). While the material is ready for use, for best results when obtaining SEM-EDS analyses, the material was dried under vacuum for 5–10 min or for 1–2 days under ambient conditions. Whether wet or dry, the silica material (**2**–silica) retains a bright blue fluorescence from the adsorbed material under UV irradiation from a lamp (photo, Fig. 5) and has “on–off” fluorescence responses with Cu^{2+} as illustrated (photo, Fig. 5, and movie file, ESI†).

Preparation of $\text{Zn}_2(\text{rslysH})_2(\mu\text{-OAc})_2$ –silica hybrid [3–silica] *via* mechanochemical methods using prepared silica gel

$\text{Zn}_2(\text{rslysH})_2(\mu\text{-OAc})_2$ was synthesized *via* the reported method.⁴⁹ A small portion of synthesized nanoparticles (50 mg, 0.832 mmol) (see above) as well as a matching amount of $\text{Zn}_2(\text{rslysH})_2(\mu\text{-OAc})_2$ (50 mg, 0.067 mmol) were mechanochemically combined by analogy to the method described above. The isolation and work-up was the same as for the hybrid system described directly above. SEM-EDS data were also obtained for this final combined fluorescent product (ESI†).

Preparation of $\text{Cu}_2(\text{rslysH})_2(\text{NO}_3)_2(\text{H}_2\text{O})_3$ –silica [4–silica] hybrid *via* mechanochemical methods using prepared silica gel

An authentic sample of this hybrid was formed to determine that it was a quenched species. Demetallation would give a ligand (**1**) that bears mild blue-green fluorescence. No fluorescence was observed under UV irradiation ($\lambda_{\text{ex}} = 365$ nm).

Preparation of $\text{Zn}_2(\text{slysH})_2\text{Cl}_2$ alumina hybrid [2–alumina] *via* mechanochemical methods using commercial alumina

A small portion of commercial Al_2O_3 (*e.g.*, 50 mg, 0.490 mmol) (Aluminum oxide 90, active, neutral, Merck) and $\text{Zn}_2(\text{slysH})_2\text{Cl}_2$ (50 mg, 0.061 mmol) were taken into a mortar and ground together mechanically (15 min) using a matching pestle under analogous conditions for those that produced **2**–silica above. The effect was the formation of a bright yellow powder with the appearance of **2**–silica after grinding. Subsequent suction filtration and rinsing with distilled water allowed for removal of unadsorbed $\text{Zn}_2(\text{slysH})_2\text{Cl}_2$ (same as for **2**–silica). Hereafter, the alumina material (**2**–alumina) retains the expected bright blue fluorescence from the adsorbed material when viewed under UV irradiation ($\lambda_{\text{em}} = 365$ nm).

Preparation of functionalized silica nanoparticle *via* sol–gel co-condensation

Silica nanoparticles were synthesized by a literature sol–gel process (Stöber method).⁵⁰ TEOS (500 μL , 2.23 mmol) and $\text{Zn}_2(\text{slysH})_2\text{Cl}_2$ (compound **2**) were dissolved into an ethanol and water mixture. After 10 min of stirring, ammonia solution (1.0 mL) was added to TEOS solution. TEOS solution remained for 1 day at room temperature. Silica nanoparticle was isolated by centrifugation (work-up) and characterized by SEM-EDS and found to have a dispersion of 100–250 nm (*vide infra*, also see ESI†).

Movie file

A 30 second movie is provided as part of the ESI.† In this movie, a portion of silica gel (50 mg, 0.833 mmol) and compound **2** (20 mg, 0.024 mmol) that were mechanochemically mixed were treated with a solution of $\text{Cu}(\text{ClO}_4)_2 \cdot 6\text{H}_2\text{O}$ (1.0×10^{-2} M).

Acknowledgements

Prof. David G. Churchill (D. G. C.) acknowledges support from Korea Science and Engineering Foundation (KOSEF) (grant no. R01-2008-000-12388-0) and the NRF (National Research Foundation) of Korea (Grant No. 2009-0070330). Mr Yonghwang Ha acknowledges the use of instrumentation at the *Water Research Laboratory* of Jungwon University (Goesan-gun Chungbuk 367-805, Republic of Korea).

Notes and references

- W. W. Zhong, *Anal. Bioanal. Chem.*, 2009, **394**, 47–59.
- C. McDonagh, O. Stranik, R. Nooney and B. D. MacCraith, *Nanomedicine*, 2009, **4**, 645–656.
- M. Liong, S. Angelos, E. Choi, K. Patel, J. F. Stoddart and J. I. Zink, *J. Mater. Chem.*, 2009, **19**, 6251–6257.
- B. J. Melde, B. J. Johnson and P. T. Charles, *Sensors*, 2008, **8**, 5202–5228.
- S. Marx and D. Avnir, *Acc. Chem. Res.*, 2007, **40**, 768–776.
- E. L. Holthoff and F. V. Bright, *Acc. Chem. Res.*, 2007, **40**, 756–767.
- H. B. Li and F. G. Qu, *Chem. Mater.*, 2007, **19**, 4148–4154.
- K. C. F. Leung, T. D. Nguyen, J. F. Stoddart and J. I. Zink, *Chem. Mater.*, 2006, **18**, 5919–5928.
- J. Guo, W. L. Yang, C. C. Wang, J. He and J. Y. Chen, *Chem. Mater.*, 2006, **18**, 5554–5562.
- J. F. Wang, C. K. Tsung, W. B. Hong, Y. Y. Wu, J. Tang and G. D. Stucky, *Chem. Mater.*, 2004, **16**, 5169–5181.
- G. Modi, V. Pillay, Y. E. Choonara, V. M. K. Ndesendo, L. C. du Toit and D. Naidoo, *Prog. Neurobiol.*, 2009, **88**, 272–285.
- E. K. Stachowiak, I. Roy, Y. W. Lee, M. Capacchietti, J. M. Aletta, P. N. Prasad and M. K. Stachowiak, *Integr. Biol.*, 2009, **1**, 394–403.
- I. Roy, M. K. Stachowiak and E. J. Bergey, *Nanomed.: Nanotechnol., Biol. Med.*, 2008, **4**, 89–97.
- F. Mancini, M. L. Bolognesi, C. Melchiorre, A. Cavalli and V. Andrisano, *J. Sep. Sci.*, 2007, **30**, 2935–2942.
- I. Klejbor, E. K. Stachowiak, D. J. Bharali, I. Roy, I. Spodnik, J. Morys, E. J. Bergey, P. N. Prasad and M. K. Stachowiak, *J. Neurosci. Methods*, 2007, **165**, 230–243.
- S. Jin and K. M. Ye, *Biotechnol. Prog.*, 2007, **23**, 32–41.
- V. N. Uversky, A. V. Kabanov and Y. L. Lyubchenko, *J. Proteome Res.*, 2006, **5**, 2505–2522.
- M. Chen and A. von Mikecz, *Exp. Cell Res.*, 2005, **305**, 51–62.
- M. T. S. Trevisan, F. V. V. Macedo, M. van de Meent, I. K. Rhee and R. Verpoorte, *Quim. Nova*, 2003, **26**, 301–304.
- A. Lekman and P. Fredman, *Neurochem. Int.*, 1998, **33**, 103–108.
- M. Bele, G. Hribar, S. Campelj, D. Makovec, V. Gaberc-Porekar, M. Zorko, M. Gaberscek, J. Jamnik and P. Venturini, *J. Chromatogr., B: Anal. Technol. Biomed. Life Sci.*, 2008, **867**, 160–164.
- G. Valensin, E. Molteni, D. Valensin, M. Taraszkiewicz and H. Kozłowski, *J. Phys. Chem. B*, 2009, **113**, 3277–3279.
- M. Remelli, D. Valensin, D. Bacco, E. Gralka, R. Guerrini, C. Miglioni and H. Kozłowski, *New J. Chem.*, 2009, **33**, 2300–2310.
- H. Kozłowski, A. Janicka-Klos, J. Brasun, E. Gaggelli, D. Valensin and G. Valensin, *Coord. Chem. Rev.*, 2009, **253**, 2665–2685.
- E. Gaggelli, Z. Grzonka, H. Kozłowski, C. Miglioni, E. Molteni, D. Valensin and G. Valensin, *Chem. Commun.*, 2008, 341–343.
- J. F. Garcia-Reyes, P. Ortega-Barrales and A. Molina-Diaz, *Anal. Sci.*, 2007, **23**, 1179–1183.
- M. Ghaedi, E. Asadpour and A. Vafaie, *Bull. Chem. Soc. Jpn.*, 2006, **79**, 432–436.
- Y. Y. Song, X. B. Cao, Y. Guo, P. Chen, Q. R. Zhao and G. Z. Shen, *Chem. Mater.*, 2009, **21**, 68–77.
- S. J. Lee, D. R. Bae, W. S. Han, S. S. Lee and J. H. Jung, *Eur. J. Inorg. Chem.*, 2008, 1559–1564.
- D. Aiello, L. Malfatti, T. Kidchob, R. Aiello, F. Testa, I. Aiello, M. Ghedini, M. La Deda, T. Martino, M. Casula and P. Innocenzi, *J. Sol-Gel Sci. Technol.*, 2008, **47**, 283–289.
- K. Sarkar, K. Dhara, M. Nandi, P. Roy, A. Bhaumik and P. Banerjee, *Adv. Funct. Mater.*, 2009, **19**, 223–234.
- A. Khan, S. Ahmed, F. Mahmood, M. Y. Khokhar and M. Riaz, *Radiochim. Acta*, 2003, **91**, 413–418.
- G. Hungerford, M. I. C. Ferreira, M. R. Pereira, J. A. Ferreira and A. F. Coelho, *J. Fluoresc.*, 2000, **10**, 283–290.
- S. H. Choi, K. Kim, J. Jeon, B. Meka, D. Bucella, K. Pang, S. Khatua, J. Lee and D. G. Churchill, *Inorg. Chem.*, 2008, **47**, 11071–11083.
- K. Kim, I. Kim, N. Maiti, S. J. Kwon, D. Bucella, O. A. Egorova, Y. S. Lee, J. Kwak and D. G. Churchill, *Polyhedron*, 2009, **28**, 2418–2430.
- S. H. Choi, K. Pang, K. Kim and D. G. Churchill, *Inorg. Chem.*, 2007, **46**, 10564–10577.
- I. Bandyopadhyay, M. J. Kim, Y. S. Lee and D. G. Churchill, *J. Phys. Chem. A*, 2006, **110**, 3655–3661.
- O. A. Egorova, O. G. Tsay, S. Khatua, J. O. Huh and D. G. Churchill, *Inorg. Chem.*, 2009, **48**, 4634–4636.
- S. Khatua, S. H. Choi, J. Lee, J. O. Huh, Y. Do and D. G. Churchill, *Inorg. Chem.*, 2009, **48**, 1799–1801.
- S. Khatua, S. H. Choi, J. Lee, K. Kim, Y. Do and D. G. Churchill, *Inorg. Chem.*, 2009, **48**, 2993–2999.
- S. Khatua, K. B. Kim, J. Kang, J. O. Huh, C. S. Hong and D. G. Churchill, *Eur. J. Inorg. Chem.*, 2009, 3266–3274.
- S. Angelos, Y. W. Yang, N. M. Khashab, J. F. Stoddart and J. I. Zink, *J. Am. Chem. Soc.*, 2009, **131**, 11344–11346.
- M. Pita, M. Kramer, J. Zhou, A. Poghosian, M. J. Schoning, V. M. Fernandez and E. Katz, *ACS Nano*, 2008, **2**, 2160–2166.
- G. J. Brown, A. P. de Silva, M. R. James, B. O. F. McKinney, D. A. Pears and S. M. Weir, *Tetrahedron*, 2008, **64**, 8301–8306.
- S. A. Krivelevich, Y. I. Denisenko and A. A. Tsyurev, *Micro- and Nanoelectronics* 2003, 2004, **5401**, 119–128.
- S. Giordani and F. M. Raymo, *Org. Lett.*, 2003, **5**, 3559–3562.
- S. Murphy, D. Boyd, S. Moane and M. Bennett, *J. Mater. Sci.: Mater. Med.*, 2009, **20**, 2207–2214.
- Z. R. Gou, W. J. Weng, P. Y. Du, G. R. Han and W. Q. Yan, *J. Biomed. Mater. Res., Part A*, 2008, **85a**, 909–918.
- S. Khatua, J. Kang and D. G. Churchill, *New J. Chem.*, 2010, **34**, 1163–1169.
- W. Stober, A. Fink and E. Bohn, *J. Colloid Interface Sci.*, 1968, **26**, 62–69.
- D. G. Churchill, *J. Chem. Educ.*, 2006, **83**, 1798–1803.